Velocity-Gated Wetting Uniformity in Confined-Tube Forced-Immersion Quenching of a Cylindrical Steel Body

Sanjana Sharma[1,*]

[1] Department of Mechanical Engineering-Engineering Mechanics, at Michigan Technological University
* Correspondence: sanjsharma@gmail.com

Abstract: The forced-quench process under consideration is one in which water delivery, vapor suppression, recirculation, and wall heat extraction occur in such a way that the outcome, namely rapid and uniform cooling sufficient for hardening treatment, results from the combined action of the four factors. This paper examines if the dependency of quenching behavior on velocity in a confined-tube quench process can be classified by the wetting characteristic associated with the wall boundary condition. The case involves quenching a stainless-steel cylinder having a diameter of 31.8 mm and length 152.4 mm heated to 870 °C with 20 °C water inside a quenching tube of diameter 107 mm and length 1000 mm using velocities of 1, 2, 4.2, and 6 m/s. The key variables include maximum vapor fraction, vapor suppression time, reattachment distance, heat flux from the wall, heat transfer coefficient, surface temperature, and cooling rate. The process transitions from insufficient performance to adequate performance when the flow eliminates both vapor shielding and generates a sufficiently lengthy recovery path along the wall. For instance, for 1 m/s of flow velocity, vapor fraction attains 29.5%, which denotes significant shielding effect. However, for a velocity of 4.2 m/s, vapor fraction decreases significantly, reaching 10%, dissipating after 1.5 s. Sidewall heat transfer coefficient exceeds 22.4 kW/(m^2 K), and the cooling rate is above 650 °C s^{-1}. For the highest velocity (6 m/s), sidewall heat flux reaches almost 18 MW/m^2 while mid-side cooling rate exceeds 1900 °C s^{-1}. Nevertheless, increasing the velocity from 4.2 m/s to 6 m/s should be considered as changing from sufficient to maximum severity levels. The research question is addressed in a direct manner by way of velocity-gated wetting, which enables the determination of the lowest velocity necessary, which, according to the research findings, would be 4.2 m/s.

Keywords: forced-immersion quenching; boiling heat transfer; wetting uniformity; confined tube; cooling rate; heat-transfer coefficient; steel heat treatment; thermal-process design

Citation: Sanjana Sharma. 2022. Velocity-Gated Wetting Uniformity in Confined-Tube Forced-Immersion Quenching of a Cylindrical Steel Body. *TK Techforum Journal (ThyssenKrupp Techforum)* 2022(1): 41–57.

Received: September-04-2022
Accepted: November-20-2022
Published: December-30-2022

1. Introduction

Forced-immersion quenching is a transformation from a flow regime to a microstructure and size effect. In steel thermal treatments, the critical stage following the contact between the heated metal surface and a cooling liquid determines the thermal profile, which governs the sequence of transformation, the hardening characteristics, residual stresses, and distortion. The engineering task does not simply lie in choosing the right fluid—water rather than oil or a high velocity—among other factors. Quench designs have to satisfy two criteria: intensity to exceed the necessary cooling-rate interval and homogeneity to prevent unwanted thermal gradients within the material. Standard heat treatment books outline the criteria as quench severity, hardenability, part geometry, agitation, and capability for maintaining an adequate heat transfer interface between the quenching medium and the solid phase [1–4].

The physical problem is posed by the non-steady nature of the convection regime, in which a steel piece initially close to 870 °C lies well above the saturation point of water. The stages in the initial quenching period can involve film boiling, transition boiling, nucleate boiling, condensation, and single-phase convection. Not all regimes occur simultaneously

over the whole surface. Orientation, impingement angle, restriction, vapor escape, and liquid renewal at the wall result in spatial and temporal variations of the heat-transfer coefficient. Heat flux undergoes abrupt changes depending on liquid-solid versus vapor insulation, local stagnation effects, subcooling, and the shape of the boiling curve [5–12].

Quenching complications multiply when the part itself becomes embedded in a channel or tube. Confined geometries tend to enhance beneficial directional guidance but also introduce recirculation and vaporization pockets that slow down wetting in specific areas. A fixed velocity value at the entrance thus does not reflect fully the thermal boundary condition experienced by the part. Observations and inverse calculations on quenching have found time and again that effective heat transfer is contingent upon agitation, section area, fluid refreshment, and surface history, meaning that a process based solely on volumetric flow rate would be too mild or too strong [13–17]. Related findings can be found in research on spray quenching, jet impingement, and cylindrical specimen cooling, where wall geometry, local wetting dynamics, and flow attachment influence heat removal [18–22].

Computational simulation opens up an approach for unraveling such coupled processes, especially when direct experimentation in the quench chamber itself proves challenging. Volume-of-fluid analysis, conjugate heat transfer, phase change, and turbulence modeling can model the onset and collapse of vapor while retaining thermal response of the solid body [23–27]. These computational techniques have seen applications to jet impingement, film boiling, droplet impact, and forced quenching, revealing that multiphase flows dominate the early stages of the quench [28–32]. Even so, two-phase simulations with sufficient resolution may not always provide the best foundation for industrial decision-making. A succinct list of wall state variables would provide engineers with information on whether a chosen velocity is too low, too high, or sufficient for a particular chamber and specimen geometry.

The confined cylindrical-tube quench tested by Moon et al., on the other hand, provides a well-defined array of geometric, thermophysical, phase-fraction, flow recovery, heat flux, heat transfer coefficient, and cooling rate data [33]. Here, the specimen is a 31.8 mm-radius by 152.4 mm-length stainless-steel cylinder; the enclosing tube has a 107 mm diameter and 1000 mm length; the starting temperature is 870 °C; and the inlet water temperature is 20 °C. Four velocities of 1, 2, 4.2, and 6 m/s were used. These velocities provide a physical basis for discriminating among the velocity values, including a low-speed case involving considerable vapor presence, middle values associated with improved wetting, and finally a high-speed case associated with maximal thermal severity. Sidewall reattachment lengths of 95, 193, 220, and 243 mm for the four velocity values illustrate the marked growth in the internal hydraulic recovery length at higher inlet momentum [33].

The design question here is whether a confined-tube forced immersion quench can be rated according to a velocity-based criterion based on wetting uniformity that takes account of vapor suppression, hydraulic flow recovery, and adequacy of the cooling rate, and how to determine the minimal adequate velocity for the geometry. In contrast to asking if increasing velocity means increasing heat transfer, the engineering question is at what point does the quench move from vapor-limited cooling to adequate thermal capability. The reason why this is an important matter is that while a severe quench could cause thermal stresses and increased pumping, inadequate thermal capability could mean insufficient hardness or even inappropriate phase transformation [34–36].

This transition has been distilled into the three observable states presented in the graphical abstract Figure 1 to form the basis of the analysis. The vapor-shielded state reigns supreme at 1 m/s, the wetting state becomes sufficient at 4.2 m/s, and 6 m/s delivers maximum heat extraction severity within the examined velocities. The graphical representation thus acts as a starting point for the investigation, with subsequent figures explaining various stages of the depicted transition, from the quench cell design all the way to the results of velocity selection.

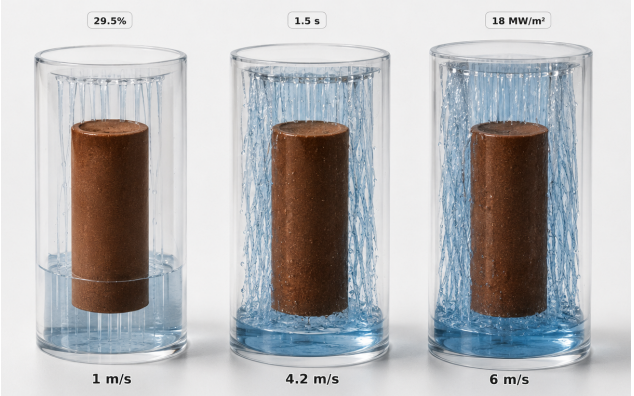

Figure 1. Velocity-gated wetting transition.

Another reason for focusing on wetting uniformity as the criterion is that the cooling rate cannot be determined based on average heat removal alone. Metal heat treatment processes are determined by the specific trajectory within the temperature-time domain. While one part of the surface cools sufficiently quickly to initiate martensite formation, another part can remain in the range for other microstructural products like bainite or pearlite formation, leading to a temperature gradient that will induce distortions even if average heat removal is satisfactory. Metallurgical literature thus treats quenching as a dual problem of thermal kinetics and structural integrity rather than as a simple optimization of heat removal [34–36]. This concern becomes relevant for the study due to the specific geometry of the problem; since the fluid stream is required to rearrange itself around the specimen's shape, the problem requires a specific set of thermal parameters such as the tube's diameter, specimen's radius and height, initial water temperature, monitoring locations, vapor fraction, heat extraction severity, etc.

The main contribution of the work lies in developing a self-contained, wall-resolved interpretation of the confined-tube quench. All the parameters including the geometry, material properties, operating temperatures, velocity window, monitoring locations, and performance measures are taken into consideration; however, the wetting process serves as a central theme instead of a single velocity value. Of particular interest is the sidewall, which shows the strongest heat extraction according to numerical data. The bottom surface is considered a delayed-wetting area rather than an immediately cooled interface.

2. Geometrical, Thermophysical Parameters, and Wall-Resolved Datas

In this quenching scenario, the system consists of a vertically enclosed cylindrical tube where the hot stainless steel specimens experience cooling with the input of water from above the domain. The geometrical details of the case are briefly explained in Figure 2. The inner diameter of the tube (107 mm) ensures that an annular channel forms between the tube and a specimen with a radius of 31.8 mm while the specimen length 152.4 mm results in different zones of interest regarding their thermal performance: top, side, and bottom sides. The measurement points MP1 to MP5 represent the top surface and the sides. These distinctions are necessary since the temperature curves suggest that there was no uniform quench process in terms of space: one observes fast quenching near the sidewall, the first impingement point on the top surface due to vapor generation, and finally, the bottom surface where the quenching occurs only after the phase arrives there [33].

The domain geometry illustrated in Figure 2 indicates that it cannot be adequately represented by one-dimensional lumped parameters. Indeed, the jet impacts the upper portion first, and then the water and vapor pass along the side clearance, and finally the liquid reaches the lower portion of the sample following its transformation by the effects of wall acceleration and recirculation. As a consequence, even if the inlet velocity is the same, different local histories occur at points MP1, MP3, MP4, and MP5. In engineering practice, different local histories mean different probability of early shielding by the vapor

film, different time when the surface enters the intense cooling stage, and different thermal gradient.

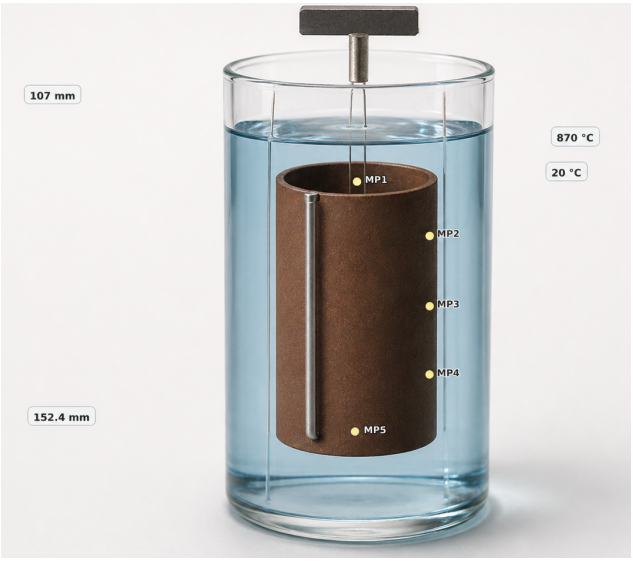

Figure 2. Confined quench cell.

Material and fluid properties chosen for the simulation are summarized in Table 1. These are the properties of the stainless steel, water, air, and vapor. The properties such as the density (7850 kg/m^3), specific heat (434 J/(kg K)), and thermal conductivity (16.5 W/(m K)) of the steel define the thermal inertia of the hot body. Water density, heat capacity, thermal conductivity, and viscosity define the properties of the cooling liquid, and the properties of air and vapor define the weakly-conductive gas stages until the wetting stage is fully reached. The most striking difference is the difference between the properties of water and vapor. The thermal conductivity of water equals 0.6 W/(m K), while the thermal conductivity of the vapor equals 0.0261 W/(m K). A vapor-rich layer therefore changes the wall boundary condition by far more than a simple adjustment of liquid velocity would suggest.

Table 1. Thermophysical inputs.

Property	Stainless steel	Water	Air	Vapor
Density, ρ (kg/m^3)	7850	998.2	1.225	0.6
Specific heat, c_p (J/(kg K))	434	4182	1006	2014
Thermal conductivity, k (W/(m K))	16.5	0.6	0.0242	0.0261
Dynamic viscosity, μ (kg/(m s))	–	0.001	1.789×10^{-5}	1.34×10^{-5}

The property set defined in Table 1 highlights the thermal asymmetry of the system. In particular, the steel component holds much sensible heat; the liquid phase is characterized by high heat capacity and much more heat transfer efficacy compared to air and vapor phases. Therefore, this process relies on the fast exchange of gas-dominant boundary layers with fresh liquid. This is the first point that allows interpreting the velocity effect as a wetting uniformity effect: any increase of velocity is good as long as it ensures the shorter vapor-dominant period and liquid wetting of the boundaries, where the heat rejection process occurs.

Wall-resolved quantities of the case are summarized in Table 2. Initially, the steel component has temperature of 870 °C, whereas water has 20 °C. The velocity range of 1–6 m/s appears to be sufficiently broad for investigating quenching behavior variation. For example, at velocity of 1 m/s, the maximal value of vapor fraction equals 29.5% meaning that a substantial part of the domain exhibits the vapor-dominant behavior at the initial time step. For 4.2 m/s, peak vapor fraction is estimated as 10%; the vapor disappears

around 1.5 s. Sidewall reattachment length increases from 95, 193, 220, to 243 mm at 1, 2, 4.2, and 6 m/s. Thermal characteristics reveal the consequences of hydraulic variation: at 4.2 m/s, the sidewall heat-transfer coefficient equals 22.4 kW/(m^2 K); the maximum heat flux reaches values of up to 18 MW/m^2 and 6 m/s; and peak sidewall cooling rate is equal to 1900 °C s^{-1} for 6 m/s [33].

Table 2. Velocity-resolved quench quantities.

Quantity	Value	Process meaning
Initial specimen temperature	870 °C	Initial thermal load of the steel cylinder
Water inlet temperature	20 °C	Reference liquid temperature for all wall cooling histories
Inlet velocities	1, 2, 4.2, and 6 m/s	Process window for weak, transitional, sufficient, and maximum-severity operation
Peak vapor fraction at 1 m/s	29.5%	Evidence of persistent early vapor shielding
Peak vapor fraction at 4.2 m/s	about 10%	Evidence of improved vapor collapse and wetting recovery
Vapor-clearance time at 4.2 m/s	about 1.5 s	Transition from two-phase-dominated cooling to liquid-dominant cooling
Reattachment lengths	95, 193, 220, and 243 mm	Hydraulic recovery scale for 1, 2, 4.2, and 6 m/s
Sidewall heat-transfer coefficient at 4.2 m/s	22.4 kW/(m^2 K)	Evidence of strong sidewall heat extraction at sufficient velocity
Top single-phase coefficient	about 10 kW/(m^2 K)	Reference post-boiling convective level near the upper surface
Maximum sidewall heat flux at 6 m/s	about 18 MW/m^2	Upper severity limit in the investigated velocity range
Peak mid-side cooling rate at 6 m/s	about 1900 °C s^{-1}	Maximum wall-cooling intensity in the velocity range
Cooling-rate threshold for hardening discussion	above 450 °C s^{-1}	Practical metallurgical reference for suppressing slower transformation paths
Cooling rate at 4.2 m/s	above 650 °C s^{-1}	Evidence that the sufficient-velocity case exceeds the hardening reference window

While the values in Table 2 supply numbers for the study's boundary conditions, they also define the very logic of the experiment. A velocity of 1 m/s cannot be considered weak because of the low inlet momentum; it is weak because of the remaining high vapor fraction showing shielding effects. A velocity of 4.2 m/s is not just an intermediate case, but also shows a strong reduction of vapor, an already high sidewall heat-transfer coefficient, and exceeding a metallurgically relevant threshold for the cooling rate. Finally, the maximum velocity of 6 m/s does not have to be optimal for manufacturing purposes per se; it is the most severe value within the velocity range and thus depends on the necessity for an extra thermal load to the component.

Furthermore, using all quantities at once eliminates quite a number of sources of uncertainties, which can weaken any study about quenching. The initial and inlet temperatures are known, hence the potential for thermal forcing is defined. The geometry of the specimen and the tube allows one to estimate how confined it is and the side clearance is present. As far as the measurement points coincide with the wall points, the local nature of the temperature history can be used in discussion. The range of velocities allows one to see both weak and strong cases of forced convection and, therefore, observe threshold behavior. Lastly, the values for vapor fraction, reattachment length, heat transfer coefficient, heat flux, and cooling rates allow one to verify the results of analysis by one of these variables in the context of others. Surface temperature cannot be used to differentiate between vapor limited behavior and weak convection, and heat transfer coefficient does not say anything about whether it has been exceeded after the necessary delay.

Similarly, the numeric foundation of the quench analysis influences confidence in its interpretation. The CFD simulation relied on two-dimensional axisymmetric geometry, volume-of-fluid formulation, conjugate heat transfer model, and Lee-type phase change model. At 4.2 m/s, grid-size and time-step tests were conducted using 190,000 quadrilateral elements and time step of 10^{-6} s. At this inlet speed, the MP4 temperature difference between the results of simulation and experiment was not more than 9.9 °C [33]. All those aspects explain why the thermal metrics are a good basis for the process selection procedure. In addition, an ability of one single set of velocities to contain vapor fraction, reattachment length, heat transfer coefficient, heat flux, temperature profile, and cooling rates is very

beneficial for detecting the point of transition from vapor-dominated quenching to liquid-controlled mechanism.

3. Wall-State Analysis Based on Velocity Gate

An interpretation of quench based on wall-state changes is analytical. According to it, the upper wall faces the first contact with water jets, while the side wall sees the acceleration of the flow and the recovering of its pathway. The bottom wall experiences delayed wetting. The evidence path in terms of the approach used in this research is shown on Figure 3, where each inlet speed is analyzed with respect to its vapor state, distance of sidewall recovery, and the cooling response. Such an interpretation does not substitute the whole simulation result but transforms it into the wetting-specific metrics.

The velocity rail in Figure 3 divides the thermal history into four coupled regimes. First, there is the regime of vapor-dominated cooling at the lowest velocity, where the gas phase causes a delay in the effective contact of water. Second, there is the partial recovery on the side walls at 2 m/s, where the reattachment length greatly increases but the complete adequacy condition is not achieved. Third, there is the sufficient state at 4.2 m/s, where vapor persistence, side wall recovery, and cooling speed are consistent with the same operation explanation. Fourth, there is the 6 m/s regime, where a higher state providing maximal thermal aggression occurs, not the first indication of sufficiency. In order to capture the strongest insight, this description is explicitly wall-resolving; the strongest information is not in the mean cooling of the sample but in the difference between walls.

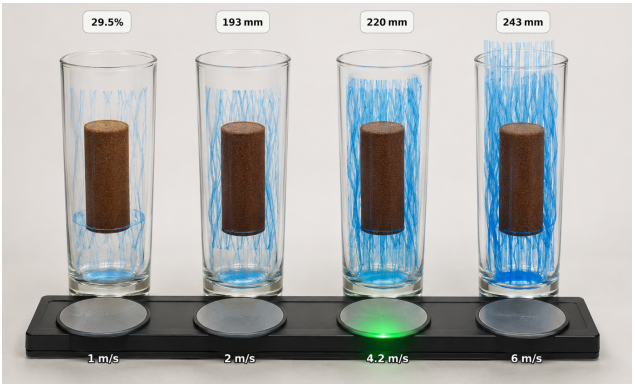

Figure 3. Velocity sufficiency boundary.

The wall-state balance from Eq. (1), employed to interpret the observations, may be expressed concisely in the form

$$M_i c_{p,s} \frac{dT_i}{dt} = -h_i(t,U) A_i (T_i - T_\infty) + \Phi_i(t), \tag{1}$$

where T_i is the effective wall temperature of position i, M_i and A_i represent the mass and area of this region of the material respectively, $c_{p,s}$ is the heat capacity of steel, U is the inlet velocity, T_∞ is the reference water temperature of 20 °C, and $\Phi_i(t)$ denotes the conductive exchange with adjacent solid regions. Since the precise values of M_i and A_i are irrelevant to this discussion because the interpretation is based on wall histories of MP1–MP5, this form of the equation is helpful in showing explicitly that quench performance is a function of the time- and velocity-dependent boundary coefficient rather than cooling coefficient.

The boundary coefficient is interpreted as the sum of a liquid convective term and a boiling term,

$$h_i(t,U) = h_{i,L}(U) + h_{i,B}(U) G_i(t,U), \tag{2}$$

where $h_{i,L}(U)$ is the liquid-dominated term, $h_{i,B}(U)$ is the amplitude of the two-phase contribution, and $G_i(t,U)$ is a wetting gate that diminishes in response to the reduction

of vapor shielding. The gate does not represent a universal law of boiling. It is a process metric that employs the vapor properties to split the quench into a vapor-affected period and a subsequent liquid-dominated period. A pronounced vapor fraction peak at low velocities implies a higher or longer gate, whereas the case of 4.2 m/s with around 10% peak vapor fraction and removal of vapor shielding after roughly 1.5 s corresponds to a considerably shorter gate.

The velocity-gated adequacy approach combines three interrelated metrics. First, there is vapor suppression, which checks whether the vapor fraction has been effectively reduced to eliminate sustained vapor shielding. Second, hydraulic recovery checks if the estimated reattachment length suggests development of a sidewall liquid flow path. Third, there is cooling sufficiency, which checks whether the temperature window is sufficiently large compared to the hardening reference rate of about 450 °C s^{-1}. All three metrics are evaluated using only the published data, without employing any tunable parameters. Such evaluation is important since each of the three metrics considered individually may provide misleading information. A high local heat flux may imply only a local effect and insufficient homogeneity; a sufficiently long reattachment length does not necessarily mean sufficient cooling; finally, crossing a cooling-rate threshold does not imply removal of vapor from the wall system.

The hydraulic recovery is characterized via a normalized recovery coordinate,

$$R_U = \frac{L_r(U) - L_r(1)}{L_r(6) - L_r(1)}, \tag{3}$$

where $L_r(U)$ is the reattachment length at velocity U. This coordinate takes a value of 0 at 1 m/s, increases to approximately 0.662 at 2 m/s, 0.845 at 4.2 m/s, and 1.000 at 6 m/s. This list is not meant as a general correlation applicable to all quench chambers. Rather, it offers a normalized value for this geometry. The data indicate that the major hydraulic recovery occurs prior to 4.2 m/s. The usefulness of R_U rests in its combination with the other two criteria; alone, it just confirms that the flow topology becomes increasingly long as the velocity increases.

At the same time, the three criteria do not allow any attempt to reduce the interpretation of the result to merely the mathematical ranking. Suppression of the vapor is regime-based, hydraulic recovery is flow-topology-based, and cooling sufficiency is metallurgy-based. An effective speed can be inadequate when it satisfies only one criterion. There could be a situation in which the reattachment region is relatively large, yet still allows some vapor that would inhibit early heat removal. Or, alternatively, the speed might create a strong local heat rate spike but not ensure that the entire area achieves sufficient cooling. Sufficiency is thus considered as convergence of evidence. Such an approach is aligned with the reality of manufacturing process design, since any process is always accepted when all criteria coincide, namely the thermal history, metallurgical intention, and repeatability requirement.

Classification of the velocity into categories is presented in Table 3. Note that the classification is somewhat qualitative rather than quantitative. According to the table, 1 m/s corresponds to a vapor-limited velocity, 2 m/s – to a transitional one, 4.2 m/s – to sufficient, and 6 m/s – to maximum severity. Such a classification allows one to make a useful manufacturing-based distinction: an increase from 1 to 4.2 m/s will alter the process wetting quality and reliability, while an increase from 4.2 to 6 m/s will mostly intensify the already sufficient quench.

The adequacy classification in Table 3 is the key organizing idea. The optimal operating regime is not determined by the maximal heat flux alone. To be used for robust hardening of the considered cylindrical part, an efficient quench should not only overcome the limit related to boiling, but also create a sufficiently long sidewall recovery zone. Moreover, the quench rate should exceed the corresponding transformation limit. Velocity 4.2 m/s is thus the lowest velocity from our list, meeting these criteria simultaneously.

Such interpretation is consistent with the available data without falling into the frequent simplification associated with a natural preference for more pumping power.

Table 3. Velocity adequacy classification.

Velocity	Wetting condition	Thermal role	Process interpretation
1 m/s	Vapor-limited	Weakest sidewall recovery	High vapor fraction shows early shielding and delayed effective liquid contact
2 m/s	Transitional	Partial recovery	Reattachment length increases strongly, but the case remains below the clearly sufficient quantity set
4.2 m/s	Sufficient	Strong recovery	Vapor collapses within seconds, the sidewall coefficient reaches 22.4 kW/(m^2 K), and cooling exceeds 650 °C s^{-1}
6 m/s	Maximum severity	Highest intensity	Peak heat flux and cooling rate reach the upper values in the velocity set, with greater thermal severity than required for the stated threshold

4. Results and Discussion

Phase changes for velocity 4.2 m/s are shown schematically in Figure 4. One can see that initially air is replaced with water, vapor appears in the vicinity of the heated surface, and further collapses because of condensation and contact action of liquid. From the physical standpoint, the main idea is that the whole period lasts relatively briefly, but determines what follows. Namely, the specimen is not subjected to convective heat transfer yet; the development of vapor decreases effective contact, whereas subcooled water and renewed flow enhance the opposite trend. This contest between both trends determines how fast the wall enters its high-efficiency cooling phase.

In accordance with the quench boiling principle, the phase sequence presented in Figure 4 corresponds to the general understanding of quench boiling. When a hot wall contacts with a cold fluid, generation of vapor becomes unavoidable. What needs to be considered, however, is whether the vapor acts as an insulating medium or can be easily cleared to facilitate strong interaction between liquid and solid. As for the case of confined tube, the 4.2 m/s flow exhibits better behavior: vapor formation takes place, but it does not form a dominant obstacle. Thus, instead of peak heat flux, vapor clearance is one of the crucial parameters that characterize the performance. Large heat fluxes would not lead to effective hardening process when vapor shields a portion of the heated surface while others remain unaffected.

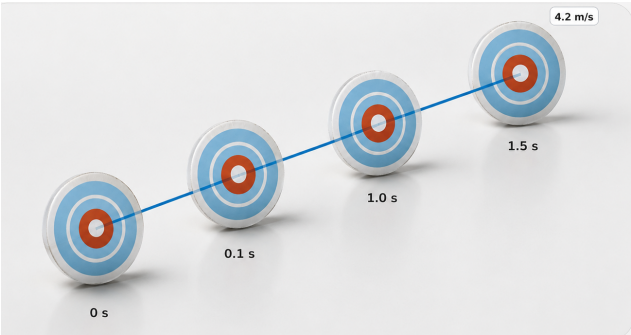

Figure 4. Early wetting chronology.

The influence of velocity on the vapor shielding effect is illustrated in Figure 5. For example, the maximum vapor fraction achieved at 1 m/s was 29.5%, whereas at 4.2 m/s it was around 10%. The latter difference cannot be overlooked since it indicates a significant alteration of the underlying heat transfer mechanism. When velocity is low, vapor fills the domain in such way that prevents direct interaction and thus leads to the prolonged period of heating. With higher flow rate, however, both convection and condensation processes become more intense; hence, vapor loses its capability of controlling the process. Clearing of the vapor phase at approximately 1.5 s at 4.2 m/s flow can be considered as the major

finding because it determines the duration of the transition period from a two-phase to liquid renewal dominated process [33].

Decreasing vapor fraction due to increasing velocity is also to be considered in relation to the initial thermal gradient. The specimen heated to 870 °C subjects the water to tremendous sensible and latent heat load on first contact. With a weak inflow momentum, the produced vapor cannot dissipate immediately, and a portion of the water entering the channel gets entrapped between the wall and a gas pocket with poor conductance. Higher inlet velocity leads to a greater capability of the liquid to flush out the gas and condense more vapor via contact with subcooled water. In addition to a more smooth curve, the result is a completely different wall situation. The heat-transfer coefficient in this case may be understood as the transient effect of a liquid film with only local two-phase interference, whereas the wall under low velocity conditions stays prone to disturbances from the unstable vapor layer.

It is easier to comprehend the weak flow regime with the help of the vapor comparison (Figure 5). While a velocity of 1 m/s brings water into the channel, there is not enough supply of the coolant to avoid an excessive initial vapor concentration. Low efficiency of cooling occurs not solely due to slow flow but because of the insulation between the hot wall and the liquid stream during the time when the steel temperature is maximum. Increasing the inlet velocity to 4.2 m/s results in better exposure of the surface to the liquid. The reasoning is confirmed by the findings from research on the impingement boiling when onset, development, and termination of contact play an important role in determining quench intensity [10–12,20].

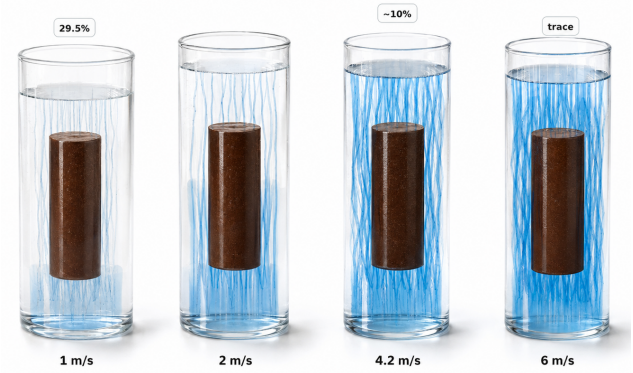

Figure 5. Vapor retreat by velocity.

Recovery of the flow on the sidewall is another interesting discovery. The reattachment lengths grow from 95 to 193, 220, and 243 mm upon increasing the flow speed from 1 to 2, 4.2, and 6 m/s, respectively. A possible explanation is presented in Figure 6. The side gap provides an acceleration zone for the vapor escape, recirculation, and new formation of the liquid film with changes in the local heat-transfer coefficient. Reattachment growth means that the flow field developing behind the upper impingement area and the side passage extends further. In the studied arrangement, the sidewall does not remain the passive zone; it becomes the area of heat action development.

Sidewall recovery's importance highlights the nature of a confined quench, in that agitation works as a renewal process in a more diffuse fashion in an open bath, with interpretation possible through generalized severity factors. In a confined space, however, the water must flow in a specific path and the separated or recirculated region behind the body's motion becomes an integral part of the heat transfer process. The increase from 95 to 193 mm as velocity increases from 1 to 2 m/s represents a significant change in flow structure. At 4.2 to 6 m/s, on the other hand, the increase of 23 mm is relatively minor, thus explaining why the higher velocity should be taken as an intensity measure, not as the start of the proper flow structure needed for heat removal.

In addition, the sidewall behavior illustrated by Figure 6 helps explain why the normalized recovery coordinate achieves a value close to 0.845 at 4.2 m/s. Much of the sidewall recovery potential that was available at the lower velocity range has been achieved up to this point. The rest of the gain from 220 to 243 mm at 6 m/s is still important but does not outweigh the earlier gain of 95 to 193 mm. In other words, a clear rationale exists to regard 4.2 m/s as the threshold point. It is not necessarily the maximum hydraulic-recovery condition but marks a crossover of the process response into the region of vigorous sidewall heat removal. Engineering-wise, the difference is meaningful as a process is thermally sufficient without being at maximum hydraulic recovery.

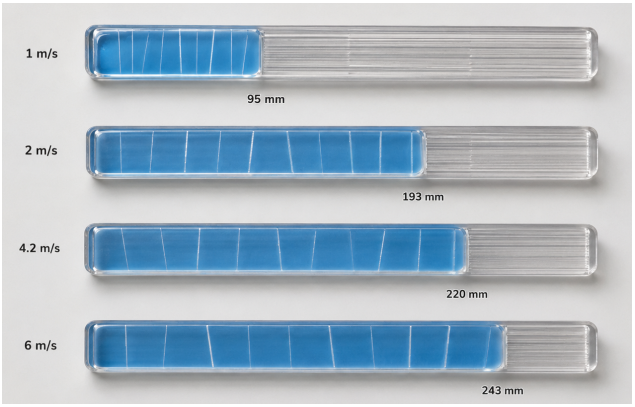

Figure 6. Sidewall recovery length.

Figure 7 provides a spatial depiction of the wall response. Given the association of the monitoring cards with MP1–MP5 in the context of thermal response, the top, sidewall, mid-side, lower sidewall, and bottom regions can be understood physically. The point MP4 bears the most prominent sidewall coefficient at 4.2 m/s and the mid-side region is tied to the greatest cooling rate response at 6 m/s. At last, the bottom indicator confirms the delayed-wetting character of the region.

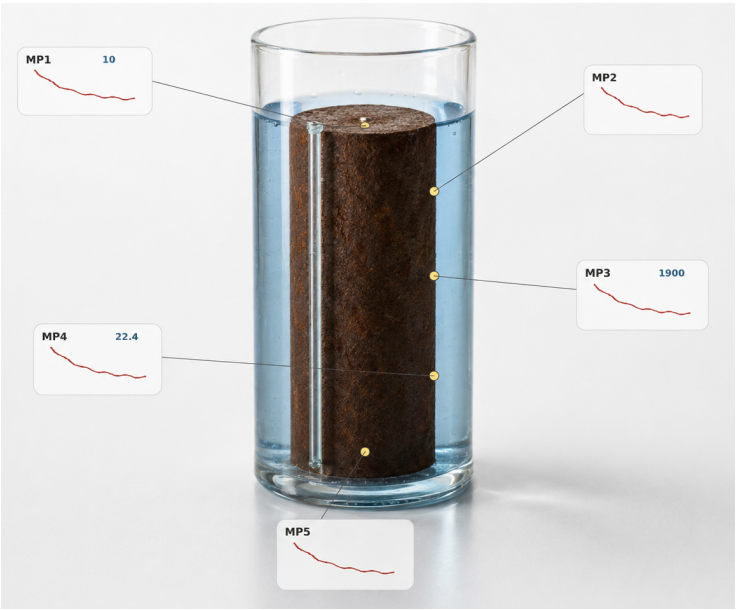

Figure 7. Local wall histories.

Wall heat flux and heat-transfer coefficients' variations are depicted in Figure8. Sidewall's reaction is extremely pronounced in comparison with that of the top, especially in MP4. The heat-transfer coefficient for the sidewall becomes 22.4 $kW/(m^2\,K)$ at a flow veloc-

ity of 4.2 m/s. In addition, at a flow velocity of 6 m/s for the sidewall, the heat flux attains a value of approximately 18 MW/m^2. These numbers suggest that there may be an area of the wall characterized by both high liquid renewal rate and good boiling-to-convection transition. As for the top, there exists a single phase post-boiling heat-transfer coefficient of 10 $kW/(m^2\,K)$. The confined geometry therefore redistributes the dominant cooling action away from a simple top-impingement picture.

An additional note is that heat flux and heat-transfer coefficient do not carry the same information about the design. The heat flux includes the current wall-fluid temperature difference, meaning it may have extremely large values in the beginning despite changes in the heat-transfer coefficient. The coefficient serves as a better indicator of effectiveness at which the surrounding fluid takes the heat away under a particular driving force. Interpreting both indicators together eliminates any misunderstandings related to high heat flux. For example, the case of 6 m/s results in the largest value of the sidewall heat flux. On the contrary, the case of 4.2 m/s possesses the highest sidewall heat-transfer coefficient and a sufficient cooling margin. In other words, both parameters must be considered when analyzing the thermal severity of the process.

The results obtained from analysis of Figure 8 demonstrate that two separate types of enhancement occur with an increase in the velocity. First of all, there is an augmentation in heat removal intensity seen as a growth in sidewall heat flux. Second, there is a stabilization of heat-transfer coefficients after the two-phase process. Stabilization is observed as a high sidewall heat-transfer coefficient at steady-state values. This aspect plays a more prominent role since it shows that the process is already dominated by the liquid flow capable of continuing to take away heat from the surface after vaporization. Thus, an isolated sharp increase is less beneficial than a smaller increase in heat flux along with stabilization of liquid heat transfer.

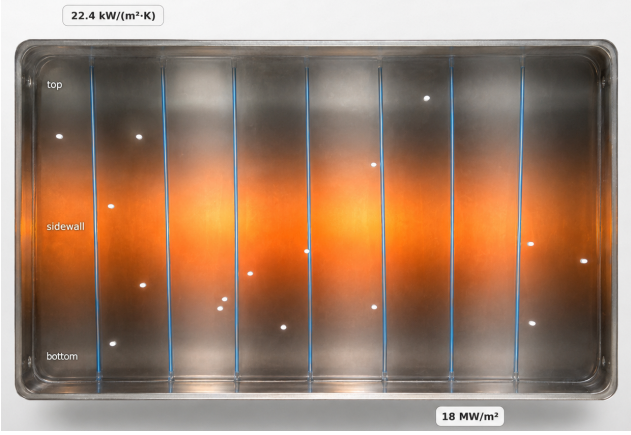

Figure 8. Sidewall heat-transfer dominance.

The nonuniformity of the heat transfer coefficient affects residual stresses and distortions as well. A large sidewall heat transfer coefficient makes it faster to form radial and axial temperature gradients within the sample at a time when the upper and lower parts have different temperature histories. Handbook for quenching points out that a higher cooling rate is not always an advantage with regard to distortion minimization [1–3]. The results obtained from the experiments with a confined tube confirm this view. The 6 m/s case demonstrates the maximum heat transfer and cooling rate; however, the highest temperatures could appear due to the most severe conditions in the range of velocities used. Therefore, the 4.2 m/s case can be recommended due to a high level of heat transfer coefficient and cooling rate without the need to apply the maximum severity.

The margin for cooling rate is illustrated in Figure 9. The diagram clearly distinguishes between the minimum satisfactory condition and maximum severity condition without assuming that the largest value represents the most favorable situation. The 4.2 m/s

condition is located above the reference of 450 °C s^{-1}, oriented on hardening processes. This condition is greater than 650 °C s^{-1}; however, the 6 m/s condition reaches about 1900 °C s^{-1}. Although the difference is rather significant, the reference curve implies severity after the necessary conditions have been satisfied. This difference may be large, but it is a difference of severity following adequacy. The reference line provides a practical interpretation in terms of cooling with the objective of hardening, wherein adequate severity would be required to prevent the formation of slow transformation products [34,35,37].

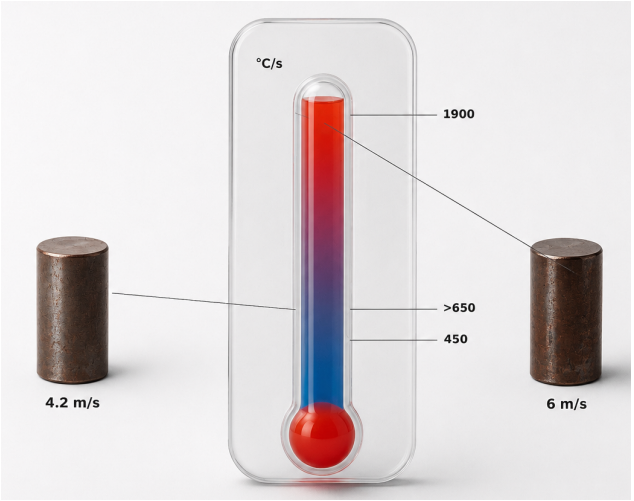

Figure 9. Cooling-rate margin.

Cooling histories in Figure 9 provide an unequivocal answer to this process selection problem. At 1 m/s, vapor fraction and cooling delay are both too large. At 2 m/s, cooling improves sidewall recovery but does not offer clear evidence that vapor has been adequately controlled and sidewall cooling rate has reached the highest margin with sidewall heat transfer coefficient close to 22.4 kW/(m^2 K). Vapor fraction decreases below threshold, vapor is extinguished in less than a second, reattachment length is close to the upper end of test values, the maximum value of the heat transfer coefficient is reached, and the cooling rate stays above 650 °C s^{-1}. Condition 6 m/s is the most severe one but has little more to offer except additional severity in comparison with the 4.2 m/s case.

Reading the temperature sequence reveals what is special about the role of the sidewall in this context. Sidewall is unique since it receives all three processes: liquid acceleration, vapor elimination, and recirculation-induced renewal. Top surface sees the incoming flow early but also gets involved in the initial vapor process, while the bottom surface heats up late because both flow development and vapor elimination require some time inside the tube. Sidewall, and more specifically, the region around MP4, thus becomes the place of transformation of momentum into heat removal. This is consistent with a relatively high coefficient at 4.2 m/s and heat flux maximum at 6 m/s. In addition, it is consistent with correlations used to describe heat exchange in turbulent forced convection for tubes [38–41].

Delayed bottom response is a factor to take into account since it is often the reason for incomplete analysis. Bottom surface in the confined tube cannot be considered as any other point where the liquid flows in equal conditions. Its temperature delay is a result of the previous stages of thermal contact of the liquid with top, sidewall, vapor and wake surfaces. In practice, a delayed bottom response may affect axial hardness variation and formation of stresses near ends and shoulders. Such consideration is more accurate since it is better to analyze monitoring points than one average sample temperature.

Wetting-uniformity criterion gives the answer to the question about the meaning of quench uniformity. All temperatures being equal in any moment of time cannot be regarded as an adequate condition of quenching uniformity. Forced immersion cannot

provide such uniformity because liquid hits various surfaces at different moments of time. Functional quench uniformity requires that the vapor is removed quickly enough, none of walls remains shielded for an extended period of time, and thermal gradients match the intended hardening path. Therefore, 4.2 m/s becomes a viable solution since it eliminates the risk of vapor shielding and allows sufficient cooling.

The relationship between cooling rate and transformation objective needs to be understood in context. Analysis here uses $450\,^{\circ}\mathrm{C\,s^{-1}}$ as a useful reference threshold, and highlights the fact that 4.2 m/s provides cooling faster than $650\,^{\circ}\mathrm{C\,s^{-1}}$. While both support a case for hardening objectives, the precise nature of the transformation for a given steel will depend on composition, initial austenite state, thickness, and appropriate CCT curve. The significance of the temperature analysis is the determination of the critical velocity that makes the quenching capable of extremely fast cooling of the surface. Then metallurgical considerations can relate that cooling history to hardness, retained austenite, distortions, and stresses of the chosen alloy.

Further conclusions demonstrate that the important physics can be captured through an appropriate combination of wall state characteristics. Quantities selected in this work do not recreate individual vortex structures and interface shapes, and they capture only the values most relevant to the manufacturing process: peak vapor fraction, vapor disappearance time, reattachment length, wall coefficient, heat flux, and cooling rate. The advantage is that, while based on numerical values, the analysis can provide decision-making in terms of the relative process strength: weak, transition, sufficient, or maximum.

One consequence of the analysis is that the most revealing period in the cycle turns out to be those first two seconds. Temperatures and coefficients beyond that time will be critical for approaching the coolant temperature, but the definitive discrimination between flow rates is established earlier in vapor reduction and wetting effects. The weak flow wastes its time while vapor protection lasts. The sufficient flow utilizes the same time frame to destroy the vapor and achieve sidewall liquid renewal. Maximum severity accelerates the response to generate a more pronounced cooling rate peak. Such a separation of the time scale makes the point relevant for control in that early time diagnostics should receive the attention rather than merely final temperature measurements of the cooled part.

It could also be expressed in terms of risk factors. Under-severity is metallurgically risky in that the surface may not cool sufficiently fast within the range of the phase transformation. Over-severity is mechanically risky due to too large gradients, excessive heat fluxes, and increased pumping capacity. The velocity 4.2 m/s takes an advantageous middle ground. Vapor clearance has taken place and strong cooling rate is achieved. Still, it does not involve the maximum heat flux within the velocity range. Therefore, the term 'adequate' is more relevant for characterization of the velocity than the term 'intermediate'. Adequacy implies the coincidence of vapor clearance, flow criteria, and heat flux criteria.

It is important to note, then, that the manufacturing interpretation is somewhat complicated. The ideal case from the standpoint of achieving maximum possible quench strength would be 6 m/s, since it has both the largest value of peak sidewall heat flux and of peak mid-side cooling rate. On the other hand, the minimum velocity that is clearly sufficient would be 4.2 m/s, since at this velocity vapor has been mostly stripped away, a lengthy recovery path has been established along the sidewall, and the heat transfer coefficient has been maximized while exceeding the adequacy cooling rate criterion by a significant margin. It should also be noted that the 6 m/s case does not necessarily represent the ideal solution for minimizing distortion [2,3,35].

In addition, these results can provide insights into the design of future experimental investigations. Obtaining measurements of all wall coefficients inside a confined quenching cell is difficult, but this study highlights which variables merit attention. The occurrence or lack thereof of vapor, the temperature history of the sidewall, reattachment-based flow recovery, and cooling rate maxima carry more weight than average outlet temperatures or overall bulk heat transfer coefficients. It is thus recommended that future experiments use combinations of visualization techniques, embedded thermocouples, and inverse

heat conduction solutions to determine whether a similar adequacy cooling rate criterion emerges [14,15,17,42].

These observations also bear on how quench quality ought to be recorded in plant trials. An outlet or final specimen temperature would overlook the early discrimination between vapor-controlled and liquid-controlled quenching. Instead, the better documentation would involve recording a short-time visualization of vapor clearing in conjunction with the temperatures indicated by at least one sidewall thermocouple at about MP4 and one additional indicator downstream from the lower wall. This approach would allow one to determine whether any fast-cooling effect observed results from wetting and/or vapor-suppression mechanisms or from an instantaneous heat flux increase in some other portion of the vessel, delaying the other areas in their heat extraction. Documentation would thus help to make informed operator training decisions.

Moreover, it supports a sound causal interpretation of what happens during the quench. The initial identification of a specific geometry and its material properties makes it possible to specify the physical system subject to cooling, the wetting-gate model allows one to explain why the first seconds of quenching matter so much, and all further discussions follow the sequence of vapor clearing, sidewall recovery, heat transfer, and rate of cooling. This causal chain avoids a common deficiency in many quenching studies in which numerical contours, coefficients, and metallurgical observations emerge seemingly unrelated to each other because the mechanism of process operation and relevant process selection criteria remain undisclosed.

5. Manufacturing Relevance and Transferability

In terms of direct relevance to practical heat-treatment operations, the analysis demonstrates the difference between velocity sufficiency and velocity maximization. Velocity sufficiency and velocity maximization represent an important distinction in production engineering but are often conflated when discussing heat transfer because the largest thermal effect tends to attract attention. In the context of an actual heat-treatment line, the optimal quench velocity will depend on hardness targets, alloy hardenability, part thickness, distortion constraints, pump energy efficiency, part geometry, and reproducibility of the cooling profile throughout the quenching run. Too low a velocity will fail to achieve adequate cooling through vapor shielding, but excessive velocity can create unnecessary thermal gradients without producing metallurgical effects.

For the confined-tube example considered above, 4.2 m/s emerges as the minimal satisfactory velocity in the velocity range because it meets all three wetting-uniformity criteria simultaneously. The conclusion does not suggest that 4.2 m/s will be satisfactory in all steels and for any quench diameter or chamber configuration. It means that, given the specified cylinder of stainless steel, the specified diameter of the tube, the specified inlet temperature, and the specified monitoring system, this particular velocity is a point where relevant parameters converge. A change of the component will retain the logic but not the numbers. The analyst needs to check that vapor shielding has occurred, that flow recovery on the wall and downstream has developed, and that the cooling intensity exceeds the required rate of transformation.

The operational interpretation is summarized in Figure 10. Four photographed quench states describe the transition from vapor-limited cooling at 1 m/s to flow recovery at 2 m/s and sufficient cooling at 4.2 m/s to maximal cooling at 6 m/s. The key idea is that 4.2 m/s represents the first velocity ensuring vapor collapse, flow recovery, and cooling-rate margin, while 6 m/s is desirable only if the increased severity is needed.

In a similar vein, hardware choices may benefit from such logic as well. In cases where a process should transition from the sufficiency criterion to a maximum severity, one way to accomplish that would be to step up the pump capacity. But there are other ways in which vapor removal and sidewall recovery could change without necessarily involving an increased bulk velocity. On the other hand, if one aims at minimizing distortion while maintaining sufficient hardening performance, then it may make sense to start from the

4.2 m/s case as the reference and then fine-tune the fixture design or agitation. The above examples demonstrate why it is better to employ the wall-resolved interpretation rather than resort to some global heat transfer number.

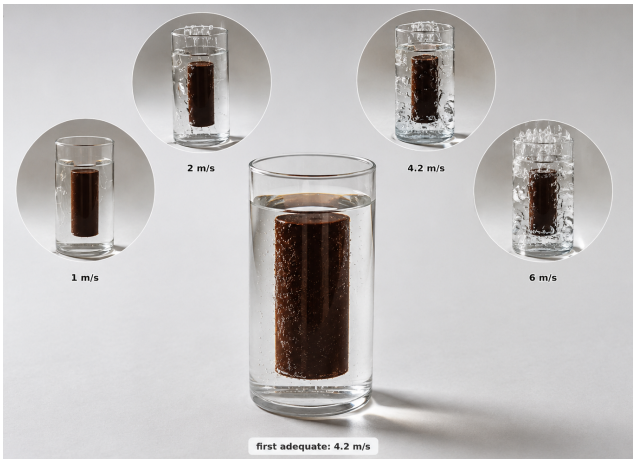

Figure 10. Quench severity states.

Finally, the wall-state approach is compatible with more thorough simulations as well. One may develop a CFD model of a different geometry and calculate all necessary quantities that could subsequently be compared against reference velocities or chambers. That is how the tasks could effectively be divided between two approaches: high-fidelity simulation captures the physics of the liquid flow, whereas the wetting uniformity approach interprets the results in terms of manufacturing.

6. Limitations

The limitations come from the quantities available at the walls and the assumptions used in the underlying axisymmetric simulation. Reduced modeling does not provide any calculations of microstructural fractions, residual stress, hardness, or distortion. Cooling-rate criteria are intended only as process-design guidance rather than a replacement of a proper continuous-cooling transformation study for a particular steel grade. Since this is a thermal analysis with stainless steel, the hardening criterion may be taken as a manufacturing requirement associated with fast cooling.

The criteria based on flow regime are affected by surface condition and coolant quality, as well. Roughness, oxidation, wettability, water chemistry, dissolved gases, and subcooling may each influence the transition between regimes of boiling, nucleate boiling, and film boiling or dry out. Experimental studies on boiling of nanofluids and wettability indicate that surface condition may affect boiling behavior even for the same nominal coolant and geometries [43,44]. For this reason, the critical threshold from simulations should be validated if the chamber will be used with another specimen surface condition or coolant quality. This criterion determines exactly what measurements need to be made to validate it: vapor fraction, reattachment length, heat transfer coefficient, and cooling rate.

The answer to the research question is clearly justified and testable. It comes from converging values of independent quantities. Vapor fraction, reattachment length, heat transfer coefficient, and cooling rate all identify the same transition from the 2 m/s case to the 4.2 m/s one. This is more significant than the value shown on any one plot, and that is why the criterion is technically defensible for design purposes and future experiments.

7. Conclusions

This work investigated whether the velocity sensitivity of the forced immersion quenching in a cylindrical tube can be understood through a criterion based on the wetting uniformity that involves the vapor suppression, the hydraulic recovery of the sidewalls, and a sufficient cooling rate. The response to the question was positive for the considered

geometry and size of the cylinder and the tube. As shown, the inlet velocity is not the key parameter in terms of design criteria. The critical velocity is that one at which increasing the flow rate suppresses the formation of vapor bubbles, enables hydraulic recovery of the walls, and increases the cooling rate to the hardening-oriented value.

The 1 m/s case is limited by vapor since its fraction peaks at 29.5%. The 2 m/s case has an improved reattachment length (193 mm), but still should be regarded as a transitional one among those available in this set. The 4.2 m/s case is the minimum critical velocity since the fraction of vapor is only around 10%, vapor evaporates already at 1.5 s, the reattachment length is equal to 220 mm, the heat transfer coefficient on the sidewall becomes 22.4 $\mathrm{kW/(m^2\,K)}$, and the cooling rate exceeds 650 $\mathrm{^\circ C\,s^{-1}}$. In turn, the 6 m/s case provides a maximal thermal severity with the peak sidewall heat flux being 18 $\mathrm{MW/m^2}$ and the peak mid-side cooling rate 1900 $\mathrm{^\circ C\,s^{-1}}$. However, the last mentioned condition is merely the intensification of quenching, not the first one that meets the criteria.

Finally, it can be concluded that the quenching with a cylindrical body in a confined tube should be designed based on the parameters concerning the uniformity of wetting and sufficient cooling rate rather than the maximal inlet velocity. For a cylindrical steel body, given tube geometry, the temperature of the water inlet, and velocities under consideration, 4.2 m/s is the critical velocity that ensures the proper quenching of steel, while 6 m/s can be considered only in extreme cases when there is a requirement for maximum severity. This approach makes it convenient to implement multi-phase thermodynamic variables for use in process selection and gives insight into the variables that need to be measured or modeled when this technique is applied to different quench tanks.

References

[1] Totten, G. E., Bates, C. E., & Clinton, N. A. (1993). Handbook of quenchants and quenching technology. ASM international.

[2] Totten, G. E. (Ed.). (2006). Steel heat treatment: metallurgy and technologies. CRC press.

[3] Liscic, B., Tensi, H. M., Canale, L. C., & Totten, G. E. (Eds.). (2010). Quenching theory and technology. CRC Press.

[4] Kobasko, N. I., Aronov, M. A., Powell, J. A., & Totten, G. E. (2010). Intensive quenching systems: Engineering and design. ASTM International.

[5] Rohsenow, W. M., Hartnett, J. P., & Cho, Y. I. (1998). Handbook of heat transfer (Vol. 3). New York: Mcgraw-hill.

[6] Pandey, V., Biswas, G., & Dalal, A. (2020). Study of Pool Boiling Through Numerical Approach. In 50 Years of CFD in Engineering Sciences: A Commemorative Volume in Memory of D. Brian Spalding (pp. 607-644). Singapore: Springer Singapore.

[7] Collier, J. G., & Thome, J. R. (1994). Convective boiling and condensation. Clarendon Press.

[8] Dhir, V. K. (1998). Boiling heat transfer. Annual review of fluid mechanics, 30(1), 365-401.

[9] Kandlikar, S. G. (2001). A theoretical model to predict pool boiling CHF incorporating effects of contact angle and orientation. Transactions-American Society of Mechanical Engineers Journal of Heat Transfer, 123(6), 1071-1079.

[10] Wolf, D. H., Incropera, F. P., & Viskanta, R. (1996). Local jet impingement boiling heat transfer. International Journal of Heat and Mass Transfer, 39(7), 1395-1406.

[11] Hall, D. E., Incropera, F. P., & Viskanta, R. (2001). Jet impingement boiling from a circular free-surface jet during quenching: Part 1—single-phase jet. J. Heat transfer, 123(5), 901-910.

[12] Hall, D. E., Incropera, F. P., & Viskanta, R. (2001). Jet impingement boiling from a circular free-surface jet during quenching: part 2—two-phase jet. J. Heat Transfer, 123(5), 911-917.

[13] LÁ? bben, T., Rath, J., Krause, F., Hoffmann, F., Fritsching, U., & Zoch, H. W. (2012). Determination of heat transfer coefficient during high–speed water quenching. International Journal of Microstructure and Materials Properties, 7(2-3), 106-124.

[14] Buczek, A., & Telejko, T. (2013). Investigation of heat transfer coefficient during quenching in various cooling agents. International Journal of Heat and Fluid Flow, 44, 358-364.

[15] Sugianto, A., Narazaki, M., Kogawara, M., & Shirayori, A. (2009). A comparative study on determination method of heat transfer coefficient using inverse heat transfer and iterative modification. Journal of Materials Processing Technology, 209(10), 4627-4632.

[16] Fernandes, P., & Prabhu, K. N. (2007). Effect of section size and agitation on heat transfer during quenching of AISI 1040 steel. Journal of Materials Processing Technology, 183(1), 1-5.

[17] Fernandes, P., & Prabhu, K. N. (2008). Comparative study of heat transfer and wetting behaviour of conventional and bioquenchants for industrial heat treatment. International Journal of Heat and Mass Transfer, 51(3-4), 526-538.

[18] Heming, C., Xieqing, H., & Jianbin, X. (2003). Comparison of surface heat-transfer coefficients between various diameter cylinders during rapid cooling. Journal of Materials Processing Technology, 138(1-3), 399-402.

[19] Puschmann, F., & Specht, E. (2004). Transient measurement of heat transfer in metal quenching with atomized sprays. Experimental Thermal and Fluid Science, 28(6), 607-615.

[20] Islam, M. A., Monde, M., Woodfield, P. L., & Mitsutake, Y. (2008). Jet impingement quenching phenomena for hot surfaces well above the limiting temperature for solid–liquid contact. International Journal of Heat and Mass Transfer, 51(5-6), 1226-1237.
[21] Mozumder, A. K., Monde, M., Woodfield, P. L., & Islam, M. A. (2006). Maximum heat flux in relation to quenching of a high temperature surface with liquid jet impingement. International Journal of Heat and Mass Transfer, 49(17-18), 2877-2888.
[22] Hosain, M. L., Fdhila, R. B., & Daneryd, A. (2016). Heat transfer by liquid jets impinging on a hot flat surface. Applied energy, 164, 934-943.
[23] Hirt, C. W., & Nichols, B. D. (1981). Volume of fluid (VOF) method for the dynamics of free boundaries. Journal of computational physics, 39(1), 201-225.
[24] Brackbill, J. U., Kothe, D. B., & Zemach, C. (1992). A continuum method for modeling surface tension. Journal of computational physics, 100(2), 335-354.
[25] Lee, W. H. (1980). A pressure iteration scheme for two-phase flow modeling. Multiphase transport fundamentals, reactor safety, applications, 1, 407-431.
[26] Launder, B. E., & Spalding, D. B. (1983). The numerical computation of turbulent flows. In Numerical prediction of flow, heat transfer, turbulence and combustion (pp. 96-116). Pergamon.
[27] Patankar, S. (2018). Numerical heat transfer and fluid flow. CRC press.
[28] Yang, Z., Peng, X. F., & Ye, P. (2008). Numerical and experimental investigation of two phase flow during boiling in a coiled tube. International Journal of Heat and Mass Transfer, 51(5-6), 1003-1016.
[29] Kim, K., & Son, G. (2013). Numerical analysis of film boiling in liquid jet impingement. Numerical heat Transfer, Part A: Applications, 64(9), 695-709.
[30] Lewis, S. R., Anumolu, L., & Trujillo, M. F. (2013). Numerical simulations of droplet train and free surface jet impingement. International journal of heat and fluid flow, 44, 610-623.
[31] Ramezanzadeh, H., Ramiar, A., & Yousefifard, M. (2017). Numerical investigation into coolant liquid velocity effect on forced convection quenching process. Applied Thermal Engineering, 122, 253-267.
[32] Stark, P., & Fritsching, U. (2015). Simulation of the impinging liquid jet cooling process of a flat plate. International Journal of Numerical Methods for Heat & Fluid Flow, 25(1), 153-170.
[33] Moon, J. H., Lee, J., & Lee, S. H. (2022). Numerical study of the boiling heat transfer characteristics of bluff body quenching in cylindrical tube. Case Studies in Thermal Engineering, 32, 101900.
[34] Porter, D. A., & Easterling, K. E. (2009). Phase transformations in metals and alloys (revised reprint). CRC press.
[35] Krauss, G. (2015). Steels: processing, structure, and performance. ASM international.
[36] Verhoeven, J. D. (2007). Steel metallurgy for the non-metallurgist. ASM International.
[37] Baumeister, T. (1967). Standard handbook for mechanical engineers. McGraw-Hill handbooks.
[38] Churchill, S. W., & Bernstein, M. (1977). A correlating equation for forced convection from gases and liquids to a circular cylinder in crossflow.
[39] Whitaker, S. (1972). Forced convection heat transfer correlations for flow in pipes, past flat plates, single cylinders, single spheres, and for flow in packed beds and tube bundles. AIChE journal, 18(2), 361-371.
[40] Huang, L., & El-Genk, M. S. (1998). Heat transfer and flow visualization experiments of swirling, multi-channel, and conventional impinging jets. International Journal of Heat and Mass Transfer, 41(3), 583-600.
[41] Nadge, P. M., & Govardhan, R. N. (2014). High Reynolds number flow over a backward-facing step: structure of the mean separation bubble. Experiments in fluids, 55(1), 1657.
[42] Barrena-Rodríguez, M. D. J., Acosta-González, F. A., & Téllez-Rosas, M. M. (2021). A review of the boiling curve with reference to steel quenching. Metals, 11(6), 974.
[43] Coursey, J. S., & Kim, J. (2008). Nanofluid boiling: The effect of surface wettability. International Journal of Heat and Fluid Flow, 29(6), 1577-1585.
[44] Li, Q., Kang, Q. J., Francois, M. M., He, Y. L., & Luo, K. H. (2015). Lattice Boltzmann modeling of boiling heat transfer: The boiling curve and the effects of wettability. International Journal of Heat and Mass Transfer, 85, 787-796.